INTERNATIONAL JOURNAL OF SCIENTIFIC RESEARCH

DISTRIBUTION OF ABSORBED DOSE IN BREAST DUE TO RADIOTHERAPY PROCEDURES WITH DIFFERENT PHOTON ENERGIES

Medical Science

A. Santamaría-Bautista	Universidad Pedagógica y Tecnológica de Colombia, Tunja, Colombia
J. S. Estepa-Jiménez	Universidad Pedagógica y Tecnológica de Colombia, Tunja, Colombia
S. A. Martinez-Ovalle*	Universidad Pedagógica y Tecnológica de Colombia. Tunja, Colombia., Centro de Cancerología de Boyacá. Tunja, Colombia *Corresponding Author

ABSTRACT

The MCNPX code was used in this work for the simulation of a treatment for breast cancer, therefore a geometry of a CT phantom (FAX06) was built through a software ImageJ which allows us to import DICOM images and then convert them into valid input files for the code. A simplified geometry of a linear accelerator (LINAC) bolster was then built, it is composed of a spherical shielding of Pb and W, and a MLC system, equivalent to those used on a VARIAN 2300 C/D. ^{60}Co, radiation beams were emitted from the center of the shielding 6 and 15 MV spectrum with an angulation to recreate the two tangential fields used in conventional treatments of breast cancer radiotherapy. The main objective of this work, was to estimate the absorbed dose in each one of the organs involved in this type of treatments. The calculation was made on a parallelized cluster, taking as reference a planification file of a conventional breast cancer treatment from a VARIAN eclipse system. The outcome permitted to establish the differences between the absorbed dose of organs in risk that are submitted like; lungs and heart, especially when different types of radiation beams are used, allowing us to establish which radiation beam is more convenient from the point of view of radiology protection to organs in risk for this treatment. The most important conclusion lies in the dose that is administered with ^{60}Co specifically in breast treatments. The almost monoenergetic energy of 1.17 MeV presents an interesting distribution with good coverage and the advantage of minimizing doses to organs at risk.

KEYWORDS

Monte Carlo, MCNPX, Radiotherapy, Breast cancer

INTRODUCTION

Cancer is a name given to a group of diseases with high social, economic and emotional repercussions, not just for the patient but for the family as well, the amount of people with such a disease and those that have died from this cause, has gradually increased in the last two years worldwide [1,2].

About 5% of the diseases in the world are related with malignant tumor in men and women in Latin America and the Caribbean, eg. There has a been a record of about 100.000 cases annually, being breast cancer in women one of the most common and the one that has increased in most of the countries in the world [3], what undoubtedly makes this malignancy worth of all kinds of investigation and research that involves not just the prevention but the implementation of treatments and techniques focused in the diminishing of deaths and the improvement of life quality in the patients.

It is very important to be able to determine the best options of a treatment. In the last decades, the prevention, discovery and the treatment of breast cancer has been transformed in such a way that more than 90 % of cases were diagnosed on an early stage and more effective treatments have been implemented such as radiotherapy (RT). After years of studies it has been demonstrated that such treatments reduce the recurrence of local rate in about 70% after mastectomy or after a more conservative treatment of breast cancer, and it could actually increase the survival on patients with a higher risk after being treated with radical surgery and systematic adjuvant treatments [4].

External radiotherapy can be provided with equipment that uses encapsulated sources of radioactive material as the ^{60}Co (cobalt therapy) which is an isotope capable of emitting gamma photons with 1.17 MeV of mainly energy. This type of equipment's rely on collimators capable of giving form and size to the beams emitted during the treatments. These type of equipment's show good results in this kind of cancer for a long time, nevertheless, the last generation of equipment's used for this procedure as the LINAC that operated under dual energies of 6 and 15 MV, 6 and 18 MV among others, have shown improvement in the consistency of the absorbed dose within the area of treatment and also a downsizing in the absorbed dose of surrounding healthy tissue. Therefore, it has displaced the conventional treatments of cobalt therapy [5]

The Monte Carlo Method has been used in different types of investigation, Eg. For the analysis of fluorescence and spectra of measured diffuse reflectance, Eg. Live mammary tissue, models that can be used to extract the properties of absorption, dispersion and fluorescence of malignant and non-malignant tissue for the diagnosis of breast cancer, all of this is based on the intrinsic properties of the tissue [6,7]. In comparative studies of dosimetry with MERT and IMRT treatments and conventional photon beams with the objective of enhancing planification systems therefore; breast cancer treatments [8], to make calculations of the absorbed energy and the absorbed dose distribution on mammary tissue for the study of the influence of mammography in the appearance of breast cancer among others. This method utilizes calculation codes to make the sampling of probability distributions, this is rooted from the realistic transportation models of radiation to make of this an instrument of scientific investigation [10]. Such procedures have demonstrated to predict the advantages and disadvantages of the techniques that involve treatments like the radiotherapy, becoming the reference technique used by the planning systems of the biggest equipment brands of radiation therapy [11].

MATERIAL AND METHODS:

The code MCNPX [12] was used for the development of this work, from which a radiotherapy procedure for breast cancer was simulated.

A patient with certain kind of phantom tomography characteristics was initially chosen to simulate the treatment. It referenced; height, weight and thickness of the patient as well as the breast size, all of this with the objective of making the simulation appear the closest to reality.

An image is taken from the eclipse system of the patient that was treated through conventional radiotherapy with a lineal VARIAN accelerator (IX) operating at 6 MV, as it is shown in Figure 1. This planning was made through two tangential fields. The objective of this work is to reproduce this treatment with a higher fidelity using photon beams of ^{60}Co, 6 and 15 MV
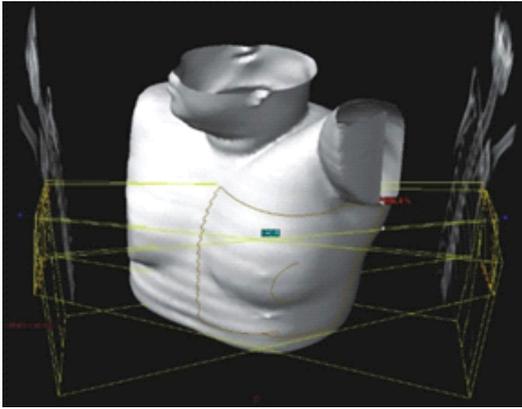
Figure 1: Planning of breast cancer treatment from left breast in Eclipse Varian system. [13].

The geometry of the female torso with all of its organs was reconstructed using software ImageJ which allowed to reproduce the FAX06 phantom [14], with voxel sizes of $3 \cdot 3 \cdot 3$ mm^3 for a total of 9057.68 cells that differ one another on their density and composition depending on which organ do the belong to according with the segmentation process that permits to visualize the geometry of the female torso within a hexahedron (Figure 2). The elemental composition of each one of the organs a tissue is taken from [15].
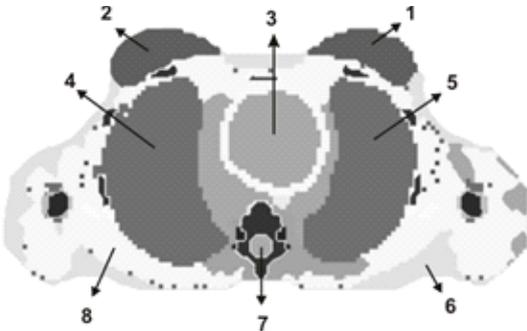
Figure 2: The tomography phantom used in the simulation. Left breast (1), right breast (2), heart (3), right lung (4), left lung (5), skin (6), marrow (7), muscle (8).

A simplified geometrical bolster is built with a linear accelerator that consist of a spherical shielding composed of two high density materials (Pb = 11.35 g·cm^3 y ρW 19.3 g·cm^3) one with a 26.75 cm radius and the second one with a 8.331 cm radius from the center of this geometry with a ^{60}Co photon spectrum and a spectrum of 6 MV and a spectrum of 15 MV. Two tangential fields were recreated to be adjusted to the planning displayed in the Figure 1, for which a multilayer system was built, (Figure 3). A total of six simulations were necessary, situating the multilayer system at 30 cm SSD for ^{60}Co and at 50 cm SSD for the 6 MV and 15 MV spectrum.
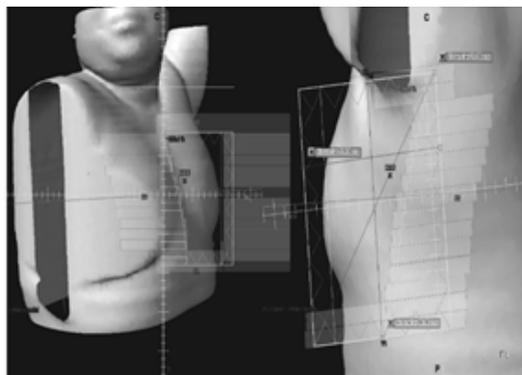
Figure 3. The image of the MLC system, planning of Eclipse reference system of VARIAN. The MLC system that reproduces the MLC position for the MCNPX code is displayed on both ends.

The complete geometry that simulates the two tangential fields (internal and external field) used in the six different calculations that are displayed in Figure 4. These calculations were based in the parallelized cluster simulating a total of $6.4.10^8$ stories for ^{60}Co, $9.6.10^8$ stories for 6 MV and $7.2.10^8$ stories for 15 MV.
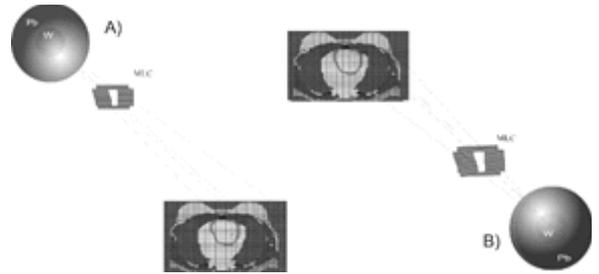

Figure 4: Complete geometry used for the simulation. A) internal tangential field. B) external tangential field.

RESULTS AND DISCUSSION:
The objective in each simulation was to study the absorbed dose in each one of the organs and tissues when they are used in the three types of beams. Having in mind that with the Monte Carlo method, the estimations are given by the emitted particle from the source. In Figures 5 and 6 the results of the absorbed dose are calculated with the tally *F8 for the three different spectra.
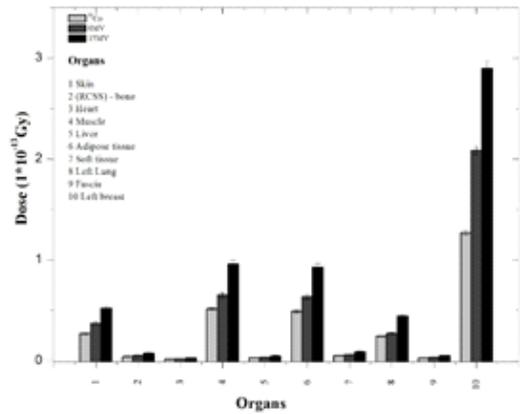
Figure 5: Absorbed dose from the internal tangential field
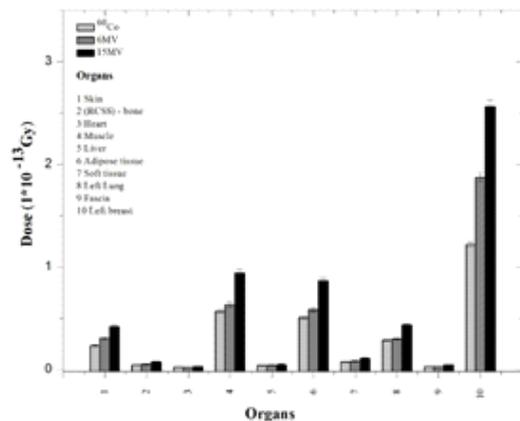
Figure 6: Absorbed dose from the external tangential field.

From Figures 5 and 6 we can observe the same behavior pattern, to more energy, more energy transference therefore more dosage. The most of contributions are given in the left mammary as expected, (10), follow by muscle (4), adipose tissue (6), skin (1), and the left lung (8), in the internal tangential field as well as the external.

On the principal diseased organs for treatment, two contributions of absorbed dose are estimated in Tables 1 and 2 to be able to show a more detailed analysis, due to the two fields as a result of the three beams of

radiation. The relative error associated to the calculation in all the cases presented below is estimated at <0.01.

As expected revising the results on Tables 1 and 2 we can observe that the absorbed dose on the left breast it is always higher than the one dosage received by the rest of the involved organs. Making a comparison between the fields, it is evident that the most contributions on the mammary are those related to the internal tangential field, nevertheless, for the rest of organs using ^{60}Co, it is higher the contribution with the external tangential field.

On a more specific manner we can observe the product of the internal tangential field, the 15 MV beam, contributes approximately a 9.64 % more of dosage to the treated mammary than the 6 MV and a 23.84 % more than the ^{60}Co, meanwhile in the case of the external tangential field, the 15 MV beam contributes 12.19 % more of dosage to this organ than the 6 MV beam, and a 23.77 % more than the ^{60}Co.

Table 1: Absorbed dose received by each organ.

Organs	External Tangential			Internal Tangential		
	^{60}Co	6 MV	15 MV	^{60}Co	6 MV	15 MV
	(Gy)			(Gy)		
Skin	2.30E-14	3.02E-14	4.17E-14	2.73E-14	3.72E-14	5.21E-14
(RCSS) – Cortical bone	4.46E-15	5.04E-15	7.27E-15	4.10E-15	4.98E-15	7.50E-15
Muscle	5.68E-14	6.31E-14	9.38E-14	5.13E-14	6.53E-14	9.60E-14
Adipose tissue	5.06E-14	5.84E-14	8.64E-14	4.91E-14	6.34E-14	9.28E-14
Heart	2.32E-15	2.01E-15	2.90E-15	1.74E-15	1.86E-15	2.56E-15
Left Lung	2.86E-14	2.97E-14	4.33E-14	2.43E-14	2.73E-14	4.45E-14
Left Breast	1.22E-13	1.87E-13	2.56E-13	1.27E-13	2.08E-13	2.90E-13

Table 2: Absorbed dose received by each organ in percentage

Organs	External tangential			Internal Tangential		
	^{60}Co	6 MV	15 MV	^{60}Co	6 MV	15 MV
	(%)			(%)		
Skin	24.24	31.84	43.93	23.42	31.90	44.68
(RCSS) – Cortical bone	26.59	30.06	43.36	24.75	30.02	45.23
Muscle	26.56	29.55	43.90	24.12	30.71	45.17
Adipose tissue	25.91	29.88	44.21	23.93	30.88	45.20
Heart	32.05	27.80	40.16	24.06	30.23	41.56
Left Lung	28.16	29.21	42.63	23.89	26.84	46.29
Left Breast	21.55	33.13	45.32	22.51	36.89	46.35

The contributions made by the external tangential field for ^{60}Co and 15 MV are higher in the case of skin, muscle, and adipose tissue, meanwhile in the 6 MV beam the contributions are less made by this field. As far as the lung concerns being one of the main organs at risk, we noted that the highest contributions of absorbed dose were the ones originated from the external tangential field on the 6 MV beam, whilst on ^{60}Co and 15 MV the internal tangential field contributions were actually higher. In the case of the heart, we noted that the absorbed dose that this organ receives is quite less on the internal and on the external tangential field. The two fields sum contribution is presented in Figure 7 and in Table 3.
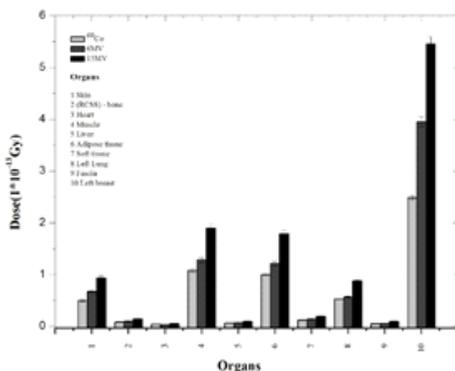
Figure 7: Absorbed dose sum due to the contributions of the two fields for ^{60}Co, 6 MV and 15 MV.

Table 3. Sum of the absorbed dose contributions for the internal and external fields

Organs	Add contributions from the two fields		
	^{60}Co	6 MV	15 MV
	(Gy)		
Skin	5.03E-14	6.75E-14	9.39E-14
(RCSS) – Cortical bone	8.56E-15	1.00E-14	1.48E-14
Muscle	1.08E-13	1.28E-13	1.90E-13
Adipose tissue	9.97E-14	1.22E-13	1.79E-13
Heart	4.06E-15	3.87E-15	5.47E-15
Left Lung	5.29E-14	5.70E-14	8.78E-14
Left Breast	2.49E-13	3.95E-13	5.46E-13

Table 4: Percentage value of absorbed dose by a particle emitted in each organ for the radiation beam of ^{60}Co.

Organs	External Tangential		Internal Tangential		Sum	
	Dose (Gy)	Dose (%)	Dose (Gy)	Dose (%)	Dose (Gy)	Dose (%)
Skin	2.30E-14	7.71	2.73E-14	9.33	5.03E-14	8.51
(RCSS) - Cortical bone	4.46E-15	1.49	4.10E-15	1.4	8.56E-15	1.45
Heart	2.32E-15	0.78	1.74E-15	0.59	4.06E-15	0.69
Muscle	5.68E-14	19	5.13E-14	17.51	1.08E-13	18.26
Liver	3.89E-15	1.3	2.85E-15	0.97	6.74E-15	1.14
Adipose Tissue	5.06E-14	16.94	4.91E-14	16.77	9.97E-14	16.86
Soft tissue	7.39E-15	2.47	5.08E-15	1.73	1.25E-14	2.11
Left lung	2.86E-14	9.58	2.43E-14	8.3	5.29E-14	8.94
Left breast	1.22E-13	40.73	1.27E-13	43.4	2.49E-13	42.05

Table 5: Percentage value of absorbed dose by a particle emitted in each organ for the radiation beam of 6 MV.

Organs	6 MV					
	External Tangential		Internal Tangential		Sum	
	Dose (Gy)	Dose (%)	Dose (Gy)	Dose (%)	Dose (Gy)	Dose (%)
Skin	3.02E-14	7.80	3.72E-14	8.91	6.75E-14	8.38
(RCSS) - Cortical bone	5.04E-15	1.30	4.98E-15	1.19	1.00E-14	1.24
Heart	2.01E-15	0.52	1.86E-15	0.45	3.87E-15	0.48
Muscle	6.31E-14	16.28	6.53E-14	15.63	1.28E-13	15.94
Liver	4.13E-15	1.06	3.35E-15	0.80	7.48E-15	0.93
Adipose Tissue	5.84E-14	15.05	6.34E-14	15.17	1.22E-13	15.11
Soft tissue	8.17E-15	2.11	6.01E-15	1.44	1.42E-14	1.76
Left lung	2.97E-14	7.66	2.73E-14	6.53	5.70E-14	7.07
Left breast	1.87E-13	48.23	2.08E-13	49.88	3.95E-13	49.08

Table 6: Percentage value of absorbed dose by a particle emitted in each organ for the radiation beam of 15 MV.

Organs	15 MV					
	External Tangential		Internal Tangential		Sum	
	Dose (Gy)	Dose (%)	Dose (Gy)	Dose (%)	Dose (Gy)	Dose (%)
Skin	4.17E-14	7.63	5.21E-14	8.71	9.39E-14	8.19
(RCSS) - Cortical bone	7.27E-15	1.33	7.50E-15	1.25	1.48E-14	1.29
Heart	2.90E-15	0.53	2.56E-15	0.43	5.47E-15	0.48
Muscle	9.38E-14	17.16	9.60E-14	16.04	1.90E-13	16.57
Liver	4.67E-15	0.85	4.79E-15	0.80	9.46E-15	0.83
Adipose Tissue	8.64E-14	15.80	9.28E-14	15.49	1.79E-13	15.64
Soft tissue	1.07E-14	1.96	8.77E-15	1.46	1.95E-14	1.70
Left lung	4.33E-14	7.93	4.45E-14	7.42	8.78E-14	7.66
Left breast	2.56E-13	46.81	2.90E-13	48.40	5.46E-13	47.64

The Table 3 displays the absorbed dose by emitted particle due to the three radiation beams. It is evidenced in this table that the beam of 15 MV in all cases presents the most of contribution of the absorbed dose.

The internal tangential field contributes on a higher percentage to the absorbed dose in the breast and skin. About (RCSS) – bone, the highest contribution is originated from the external field. In the lung the contributions are higher in the internal tangential field and higher from the external tangential field on the heart. It is important to note than on the treated organ, 15 MV contributes $2.97 \cdot 10^{-13}$ Gy more of absorbed dose than the ^{60}Co and $1.51 \cdot 10^{-13}$ Gy by emitted particle more than the 6 MV beam.

Finally, in the Tables 4, 5 and 6 we see the results in an independant form for each one of the beams. It is analyzed that the total of the absorbed dose is conveyed in each one of the spectrums for each organ.

It is evidenced which product of the internal tangential field, the 6 MV beam contributes approximately a 1.48 % more of absorbed dose to the treated mammary than the 15 MV beam and a 6.48 % more for ^{60}Co. In the case of the external tangential field, the 6 MV beam contributes a 1.42 % more of absorbed dose for this organ than the 15 MV beam and a 7.53 % more than the ^{60}Co.

In the case of skin, muscle and adipose tissue there are also higher contributions made in the internal tangential field, particularly those originated from ^{60}Co, having in mind that; these are superficial organs and that ^{60}Co contains the most part of the radiation on surface. As far as the lung concerns, one of the main organs at risk, we have noted that the highest contributions of absorbed dose were the ones originated from the external tangential field, finding again that they are higher for ^{60}Co which contributes a 1.82 % more of absorbed dose than the 6 MV beam and a 1.57 % more than the 15 MV. In the case of the heart we noted that the absorbed dose this organ receives is a minimum dose for the internal tangential field as well as for the external, having in mind the great quantity of simulated particles.

CONCLUSIONS:
The amount of absorbed dose that the different organs receive during treatment, is directly proportional to the energy of the radiation beam, finding that less quantity of dosage is transfered to the organs at risk with a ^{60}Co beam. This conclusion is left to the consideration of the manufacturers about the possibility of building an equipment of radiotherapy that uses ^{60}Co and that counts with the MLC systems.

The calculation models of absorbed dose implemented by the different manufacturers of LINAC´s, use dosimetric algorithms like; AAA, AXB, DVO, PGO and PRO, nevertheless, it is very difficult to exceed the accuracy that we have with the Monte Carlo method to be able to establish with higher precision the absorbed dose due to the interaction of the matter radiation. It remains to calculate the absorbed dose on a IMRT treatment in which different Gantry angulations interact and different positions of the MLC system are present in just one field, this makes it hard to calculate for this kind of radiotherapy.

The results found are according to the physics involved in the interaction of photons with organs and tissue, showing evidence of the advantages of using one after another radiation beam, nevertheless it is also clear that the thickness of the organ to irradiate, plays a transcendent role in the treatment and it is also evident the advantages that a procedure of radiotherapy for breast cancer with the use of ^{60}Co would have.

In organs like; skin, muscle and adipose tissue, the ^{60}Co is the one that provides a higher percentage of absorbed dose, this is due to the fact that they are superficial organs and that the energies of ^{60}Co transfer a higher energy on the first centimeters of tissue, besides it is important to note that the most contributions of absorbed dose to the different organs correspond to the external tangential field.

The most important conclusion lies in the dose that is administered with ^{60}Co specifically in breast treatments. The almost monoenergetic energy of 1.17 MeV presents an interesting distribution with good coverage and the advantage of minimizing doses to organs at risk.

The Energy of 1.17 MeV is optimal in treatments of low thickness such as breast, head and neck, in this sense it would be interesting to think of cobaltotherapy with systems (MLC) as those used by the LINACs and planning systems for these devices, this advantage saves money to the manufacturer and the user for the high costs involved in maintaining a LINAC

REFERENCES
[1] Lewis. F. M. (1986). The impact of cancer on the family: a critical analysis of the research literature. Patient Education and Counseling. 8(3). 269-289.
[2] Torre. L. A.. Bray. F.. Siegel. R. L.. Ferlay. J.. Lortet–Tieulent. J.. & Jemal. A. (2015). Global cancer statistics. 2012. CA: a cancer journal for clinicians. 65(2). 87-108.
[3] Lozano-Ascencio. R.. Gómez-Dantés. H.. Lewis. S.. Torres-Sánchez. L.. & López-Carrillo. L. (2009). Tendencias del cáncer de mama en América Latina y el Caribe. Salud pública de México. 51. s147-s156.
[4] Gomez-Iturriaga. A.. Moreno-Jimenez. M.. & Martinez-Monge. R. (2008). Tratamiento radioterápico del cáncer mama: estándares y nuevas tendencias. Irradiación parcial acelerada de la mama.
[5] Adams. E. J.. & Warrington. A. P. (2014). A comparison between cobalt and linear accelerator-based treatment plans for conformal and intensity-modulated radiotherapy. The British journal of radiology.
[6] Zhu. C.. Palmer. G. M.. Breslin. T. M.. Harter. J.. & Ramanujam. N. (2008). Diagnosis of breast cancer using fluorescence and diffuse reflectance spectroscopy: a Monte-Carlo-model-based approach. Journal of biomedical optics. 13(3). 034015-034015.
[7] Palmer. G. M.. Zhu. C.. Breslin. T. M.. Xu. F.. Gilchrist. K. W.. & Ramanujam. N. (2006). Monte Carlo-based inverse model for calculating tissue optical properties. Part II: Application to breast cancer diagnosis. Applied optics. 45(5). 1072-1078.
[8] Ma. C. M.. Ding. M.. Li. J. S.. Lee. M. C.. Pawlicki. T.. & Deng. J. (2003). A comparative dosimetric study on tangential photon beams. intensity-modulated radiation therapy (IMRT) and modulated electron radiotherapy (MERT) for breast cancer treatment. Physics in medicine and biology. 48(7). 909.
[9] Delis. H.. Spyrou. G.. Tzanakos. G.. & Panayiotakis. G. (2005). The influence of mammographic X-ray spectra on absorbed energy distribution in breast: Monte Carlo simulation studies. Radiation measurements. 39(2). 149-155.
[10] Rojas. L. (2005). El MÉTODO MONTECARLO en dosimetría y otras aplicaciones. Contacto Nuclear. 39. 14-19.
[11] Verhaegen. F.. Nahum. A. E.. Van De Putte. S.. & Namito. Y. (1999). Monte Carlo modelling of radiotherapy kV x-ray units. Physics in medicine and biology. 44(7). 1767.
[12] Pelowitz, D. B. (2005). MCNPXTM user's manual. Los Alamos National Laboratory, Los Alamos.
[13] https://www.varian.com/oncology/products/software/treatment-planning/eclipse-treatment-planning-system
[14] Kramer, R., Khoury, H. J., Vieira, J. W., & Lima, V. J. M. (2006). MAX06 and FAX06: update of two adult human phantoms for radiation protection dosimetry. Physics in medicine and biology, 51(14), 3331.
[15] Martínez–Ovalle. S. A., Barquero. R.. Gómez–Ros. J. M.. & Lallena. A. M. (2012). Neutron dosimetry in organs of an adult human phantom using linacs with multileaf collimator in radiotherapy treatments. Medical Physics. 39(5). 2854-2866.